Hindawi
International Journal of Antennas and Propagation
Volume 2017, Article ID 9096217, 6 pages
https://doi.org/10.1155/2017/9096217

Research Article

Power Link Optimization for a Neurostimulator in Nasal Cavity

Seunghyun Lee,[1] Jonghoek Kim,[2] and Sanghoek Kim[1]

[1] *Department of Electronic Engineering, Kyung Hee University, Seoul 17104, Republic of Korea*
[2] *Agency for Defense Development, Daejeon, Republic of Korea*

Correspondence should be addressed to Sanghoek Kim; sanghoek@khu.ac.kr

Received 20 March 2017; Revised 30 May 2017; Accepted 6 June 2017; Published 11 July 2017

Academic Editor: Luciano Tarricone

Copyright © 2017 Seunghyun Lee et al. This is an open access article distributed under the Creative Commons Attribution License, which permits unrestricted use, distribution, and reproduction in any medium, provided the original work is properly cited.

This paper examines system optimization for wirelessly powering a small implant embedded in tissue. For a given small receiver in a multilayer tissue model, the transmitter is abstracted as a sheet of tangential current density for which the optimal distribution is analytically found. This proposes a new design methodology for wireless power transfer systems. That is, from the optimal current distribution, the maximum achievable efficiency is derived first. Next, various design parameters are determined to achieve the target efficiency. Based on this design methodology, a centimeter-sized neurostimulator inside the nasal cavity is demonstrated. For this centimeter-sized implant, the optimal distribution resembles that of a coil source and the optimal frequency is around 15 MHz. While the existing solution showed an efficiency of about 0.3 percent, the proposed system could enhance the efficiency fivefold.

1. Introduction

Efficient wireless power transfer to medical implantable devices is highly desirable. Removal of bulky energy storage components enables the miniaturization of devices and eliminates the need for additional surgeries to replace the battery. Instead of a battery, a receiver on the implant obtains energy provided by external sources. Among various means to deliver power wirelessly, such as using ultrasound, optical, or biological sources, wireless powering through radiofrequency (RF) electromagnetic waves is the most established [1–5].

Most studies using electromagnetic waves for powering implantable devices utilize *inductive* coupling. Under these conditions, a coil structure is most commonly used as the source. In an effort to enhance the efficiency, resonant LC tanks have been used on both coils for impedance matching [4, 6]. Instead of using separate capacitors, one may use extra coils to match the impedance and maintain a high Q-factor [7].

As another effort to increase the efficiency, the size and number of turns of a coil are tuned to maximize the power transfer efficiency [3, 8]. In most studies, the optimization is based on the mutual inductance relation between two coil structures [9]. This approach, however, relies on quasi-static approximation in which the electric field induced by time-varying magnetic field is ignored. Dissipated power loss in tissue due to the presence of electric field, therefore, cannot be correctly accounted for.

Recently, optimization of the power transfer efficiency including tissue loss was performed based on full-wave analysis [10, 11]. It showed that, for any given receiver, the power transfer efficiency is upper-bounded because of the tissue loss, and the upper bound is analytically solvable. Specifically, for an implant with a size of few millimeters, the optimal frequency lies in the low gigahertz range [12]. At such a high frequency, the implant is no longer in the near-field regime from the source; hence, inductive coupling alone is not sufficient to explain the performance [13].

This finding is the basis for a new design methodology of power delivery systems. For a given receiver, one can readily obtain achievable power transfer efficiency and design the overall system to meet the goal. The power transfer efficiency can often be increased dramatically compared to those of conventional inductive coupling mechanisms [10, 11]. Equipped with this highly efficient power delivery system, a millimeter-sized pacemaker has been built and tested in a rabbit [14].

In this work, we apply the optimization technique for a few-centimeters-sized implantable device. This research is

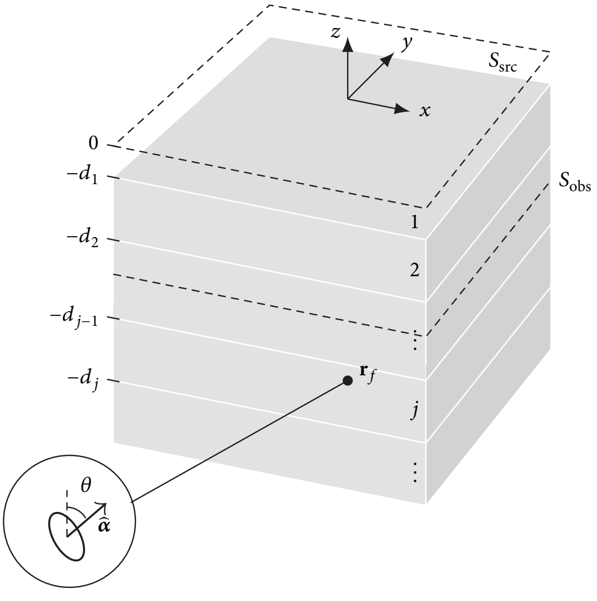

FIGURE 1: The layered medium model for tissue consists of n stacked layers, each of which is assigned a dielectric permittivity ϵ_{rj}. The center of the source is positioned at the origin, and the receiver is placed at $\mathbf{r}_f = (0, 0, -z_f)$ with the norm of $\hat{\boldsymbol{\alpha}}$ in the layers.

novel and important because most implantable devices are still of a size of a few centimeters. This work provides the maximum achievable efficiency for the receivers at a certain depth of tissue composition. As a specific application, the optimization was applied for a neurostimulator inside the cavity of the head [15]. The implant stimulates the sphenopalatine ganglion (SPG), a nerve bundle located behind the nose, to relieve the pain caused by cluster headache. For the same receiver size, our design methodology could improve the efficiency fivefold compared to previous design performance.

2. Background Theory

2.1. Power Transfer Efficiency. The power transfer efficiency is defined as the ratio between the received power P_r and the input power P_{in} to the system.

$$\eta = \frac{P_r}{P_{\text{in}}}. \quad (1)$$

Power efficiency degrades because of various factors, such as ohmic loss P_{ohm} due to finite conductivity of the source, radiation loss P_{rad}, and dielectric loss P_{tissue} inside the lossy tissue. Among those, the ohmic loss and the dielectric loss often dominate the power loss in a system. The upper bound on $\eta_{\text{tissue}} = P_r/P_{\text{tissue}}$ for a given receiver structure can be analytically solved [11]. Obviously, this forms the upper bound for the power transfer efficiency.

2.2. Tissue, Source, and Receiver Model. We model the inhomogeneity of the tissue as a planar multilayered medium, as illustrated in Figure 1. Although actual tissue medium is not a strict planar structure, it is known that planar modeling is adequate to predict the power transfer efficiency [16]. The tissue properties are modeled by assigning a dielectric permittivity ϵ to each layer. The dependence of ϵ with frequency is obtained from the Debye relaxation model [12].

Over the planar structure, we look for a source that maximizes the power transfer efficiency. It is difficult, however, to optimize the source, since the shape of the source can be arbitrary in three-dimensional space. The problem can be greatly simplified by invoking the *equivalence principle* [17], according to which any arbitrary source can be represented by an equivalent surface (tangential) current density, $\mathbf{J}_1$, along a plane S_{src} between the source and the medium, as shown in Figure 1. For the sake of convenience, S_{src} is assumed to be placed at $z = 0$.

As a result, without loss of generality, we model the source with surface electric current $\mathbf{J}_1$ on S_{src} in the rest of the paper:

$$\mathbf{J}_1(\mathbf{r}) = J_{1x}(\mathbf{r}_s)\,\delta(z)\,\hat{\mathbf{x}} + J_{1y}(\mathbf{r}_s)\,\delta(z)\,\hat{\mathbf{y}}, \quad (2)$$

where $\mathbf{r}_s = x\hat{\mathbf{x}} + y\hat{\mathbf{y}}$. Finally, the receiver of miniature devices is modeled as a magnetic dipole with arbitrary orientation $\hat{\boldsymbol{\alpha}}$ located at $\mathbf{r}_f = (0, 0, -z_f)$ (Figure 1):

$$\mathbf{M}_2(\mathbf{r}) = i\omega\mu A_r I_2 \delta\left(x, y, z + z_f\right)\hat{\boldsymbol{\alpha}}, \quad (3)$$

where $A_r I_2$ is the magnetic moment of the dipole and $\hat{\boldsymbol{\alpha}}$ denotes the orientation of the magnetic dipole, which is tilted by θ from the z-axis. For a given $\mathbf{r}_f$ and $\hat{\boldsymbol{\alpha}}$, we want to find $J_{1x}(\mathbf{r}_s)$ and $J_{1y}(\mathbf{r}_s)$ that optimize the power transfer efficiency.

2.3. Efficiency Optimization. For the given magnetic dipole moment $\mathbf{M}_2$, power transfer occurs through the time-varying magnetic field component in the direction of the moment. In a phasor notation, the transferred power is

$$P_r = \frac{\omega}{2}\,\mathrm{Re}\int d^3r\,\mathbf{M}_2^* \cdot \mathbf{B}_1, \quad (4)$$

where $\mathbf{B}_1$ is the magnetic field generated by the source $\mathbf{J}_1$ and $\mathrm{Re}\,z$ represents the real part of a complex number z. The electric and magnetic fields generated by a time-harmonic current density $\mathbf{J}_1$ on the surface of the source conductor can be solved by decomposing the current density into its spatial frequency components. Finally, the efficiency can be written as [14]

$$\eta_{\text{tissue}} = \frac{\left|\int d^3r\,\mathbf{M}_2^* \cdot \mathbf{B}_1\right|^2}{\left[\int d^3r\,\mathrm{Im}\,\epsilon(\omega)\left|\mathbf{E}_1\right|^2\right]\left[\int d^3r\,\mathrm{Im}\,\epsilon(\omega)\left|\mathbf{E}_2\right|^2\right]}, \quad (5)$$

where $\mathbf{E}_1$ and $\mathbf{E}_2$ are the electric fields generated by the source $\mathbf{J}_1$ and $\mathbf{M}_2$, respectively. Also, $\mathrm{Im}\,z$ represents the imaginary part of a complex number z. The above equation of efficiency is intrinsic to the fields in the tissue multilayer structure, excluding any power loss due to radiation or ohmic loss in the source. Therefore, this gives the upper bound on the efficiency that can be obtained. The choice of $\mathbf{J}_1$ that maximizes (5) is the key to efficient power transfer. Remarkably, the solution to the optimization problem maximizing $\eta_{\text{tissue}}(\mathbf{J}_1)$ can be found in a closed form as a consequence of vector space structure of fields in the multilayer geometry of the medium [11].

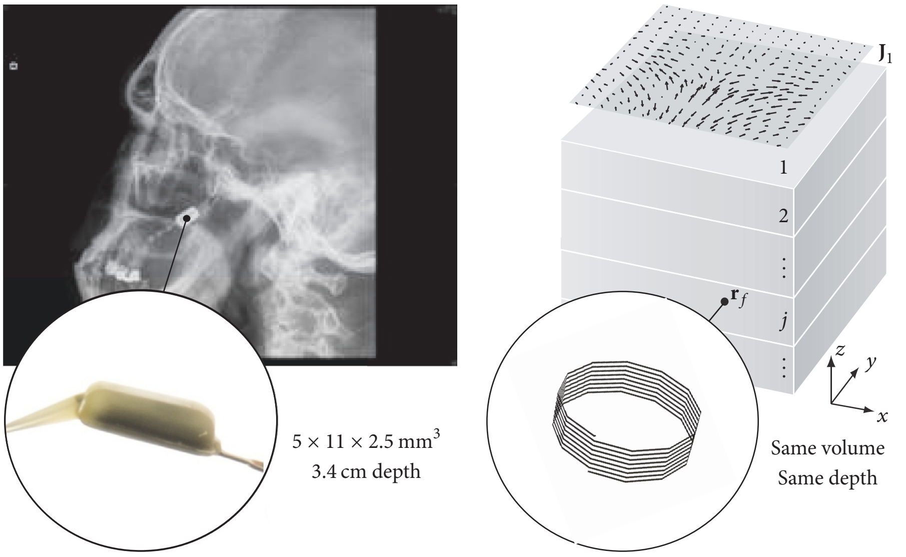

(a) (b)

Figure 2: (a) The neurostimulator implant inside the head to relieve headache pain. (b) Modeling of the receiver occupying the same volume and in the same position as the neurostimulator implant.

Table 1: Tissue composition used for the neurostimulator. The receiver is placed at 3.4 cm below the air-tissue interface (layer 5). The unit for the thickness (Δd) is millimeters.

Layer 2		Layer 3		Layer 4		Layer 5		Layer 6		Layer 7	
Tissue	Δd	Tissue	Δd	Tissue	Δd	Tissue	Δd	Tissue	Δd	Tissue	Δd
Skin	1	Muscle	22	Bone	2	Muscle	11	Bone	1	Muscle	∞

3. Application: Receiver in Nasal Cavity

A minimally invasive implantable device demands as small a size as possible. However, if the functions of an implant necessitate large amounts of power, the size of the receiver must reflect this requirement. In some cases, a relatively large implant can utilize a preexisting vacant space inside the human body and thus bypass the need for further miniaturization.

A good example of such an occurrence is a commercial neurostimulator inside the head to relieve the pain caused by cluster headache, as shown in Figure 2(a), produced by Autonomic Technologies (ATI) [15]. The implant requires a large amount of power (~50 mW) to provide intense stimulation to the sphenopalatine ganglion (SPG), a nerve bundle located behind the nose. Therefore, miniaturization of the receiver is limited by the device power consumption. Fortunately, exploiting the nasal cavity for the placement of the cm-scale implant, 50 mW of power can be delivered to the cm-scale implant in a relatively noninvasive manner.

However, despite the large size of the receiver, the system suffers from low power transfer efficiency. The existing power transfer system attempted minimization of absorption loss in tissue by operating in the range of hundreds of kHz. A Litz wire structure is adopted in the receiver to reduce the ohmic loss of the receiver, as in [7]. Nevertheless, small receiver size and long distance between transceivers reduce the efficiency significantly. As a result, the power transfer efficiency is about 0.3% for the existing wireless powering solution.

We are interested in the improvement in power transfer efficiency without increasing receiver size. In order to determine this, we model the receiver as a multiturn loop occupying the same volume as the original receiver and place it at the depth at which the implant will be located, 3.4 cm below the air-tissue interface, as in Figure 2(b). Detailed composition of tissue found from the anatomy of human is tabulated in Table 1. The thickness of the last layer is assumed to be infinite to simplify the calculation. This simplification is justified because the signal reflection from deeper layers is negligible. Following the theory in Section 2, the bound on efficiency is calculated as the black curve in Figure 3 for this receiver structure and configuration. Note that the frequency sweeping ends early at tens of MHz, after which the receiver is not modeled as a subwavelength (electrically small) structure. Equation (3) does not hold when the dimensions of the structure become comparable to the wavelength.

The optimal source that achieves the bound on efficiency in the frequency range from 100 kHz to 10 MHz is shown in Figure 4(a). It resembles a single rotational source and can be easily synthesized as a loop source, as in Figure 4(b). However, the simulated efficiency of a loop source made of copper using a commercial EM simulation tool [18] (blue curve in Figure 3) shows a vast departure from the

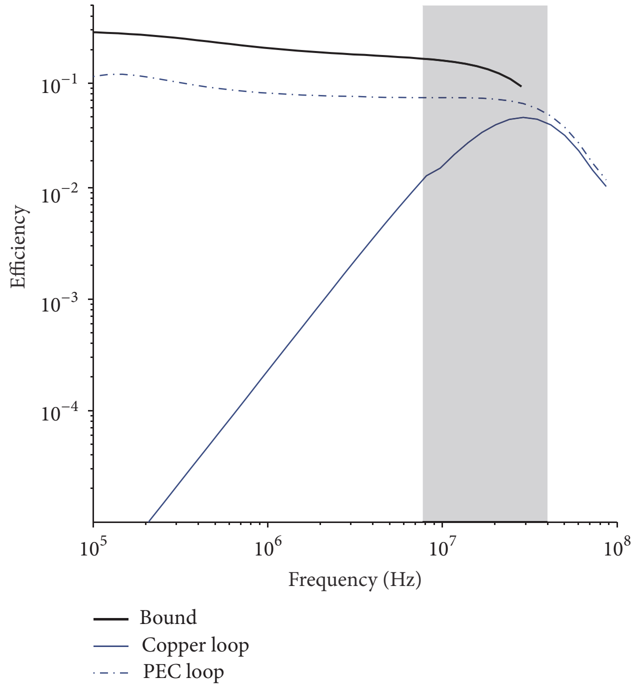

FIGURE 3: The bound on efficiency for the given receiver is shown with a solid black curve. Due to the finite conductivity of copper, the efficiency of the loop (solid blue) is much lower than the bound. To achieve an efficiency as close to the bound as possible, the device should operate in the shaded frequency range.

theoretical bound due to the finite conductivity of copper. While the ohmic loss in the source is taken into account in the simulation of the loop source, the theoretic bound considers only the dielectric loss in tissue as the loss in the system. If the material of the source is replaced by a perfect conductor (PEC), the efficiency of the loop source borders the bound as expected (dashed blue curve in Figure 3).

Without a PEC in hand, we aim to build a copper source possessing an efficiency that approaches the bound as close as possible. Therefore, the operating frequency should be chosen to be around 15 MHz (shaded region in Figure 3) to achieve the desired efficiency.

4. Experiment

An experiment is performed to measure the power transfer efficiency to the implant inside the tissue and to verify the theoretical and the simulated results. The optimal source is realized with a multiturn loop, as shown in Figure 4(c). A matching circuit is included to match the impedance of the loop to the output impedance of a power source instrument, 50 Ω, at 15 MHz.

The receiver is implemented with a multiturn loop, as shown in Figure 5(a), fitting inside the same cover used in the existing product [15]. The circuit model for the receiver is shown in Figure 6, in which the capacitance values for the rectifier are specified. The multiturn loop in a receiver can be modeled as an induced alternating voltage source V_s connected with resistance R_s and L_s. Unlike the resistance R_s, the inductance L_s of the receiver coil is not sensitive to the surrounding medium. The inductance L_s, therefore, can be easily measured using a network analyzer when the receiver is outside the tissue. The inductance of the loop $L_s = 5.9\,\mu\mathrm{H}$ could be successfully resonated out with $C_p = 15\,\mathrm{pF}$ and the rectifier.

As turkey breast mimics the tissue structure of the human cheek (Figure 5(c)), it is used as the experimental substrate. The receiver is inserted 3.4 cm into the turkey breast. The available received power can be deduced by $V_s^2/(8R_s)$ in Figure 6. The measurement of V_s and R_s, however, is challenging for small-scale structures. For example, to measure R_s, the standard method to use the deembedding structure is not suitable when the size of the deembedding structure is comparable to the structure of interest. The electromagnetic coupling between the deembedding structure and the structure of interest degrades the measurement accuracy.

Instead, an optical approach has been proposed [19]. It makes use of the nonlinearity of the rectifier to accurately characterize power receiving structures. For this purpose, an LED and the charge pulse control unit to drive the LED are included in the receiver. In this method, the LED blinking period is closely related to the amount of received power. Explicitly, by measuring the LED blinking periods for two distinct input power levels, we can estimate R_s and deduce the available received power [14, 19]. The LED blinking period is measured outside the tissue through an optical cable connecting the LED and the National Instruments (NI) machine (Figure 5(b)). The measured power transfer efficiency is then calculated as the ratio between the input power and the received power.

The result of measurement is shown in Figure 7. In the measurement, to make the LED blinking at a designated period indicating that the available power at the receiver is 0.1 mW, the transmit power was needed to be 2.85 mW. From this ratio, the available power transfer efficiency is measured to be 3.5% and denoted by a red dot in Figure 7. It shows that the efficiency closely matches the simulation result. In practice, the efficiency should degrade further during the AC-DC conversion in a rectifier. In this experiment, the AC-DC conversion efficiency is about 44% due to the small power level. This results in the overall power transfer efficiency from the input source to the load being 1.5%. Nevertheless, this is five times higher efficiency than that of the existing solution, which is denoted by a blue dot. The existing solution exceeds the simulation results (blue curve) at corresponding frequency (~800 kHz) because a Litz wire is used [15] instead of a plain coil, as was used in simulation. As stated in Section 3, Litz wire has a reduced AC resistivity and hence improves the efficiency. However, Litz wire typically has a resonant frequency of a few MHz and cannot be used for our new operating frequency. Our design methodology demonstrates that it is a better choice to discard the Litz wire and increase the operating frequency. This yields much higher efficiency than the existing solution. In other words, by following the design methodology driven by the bound provided by the theory, one can dramatically improve the power transfer efficiency.

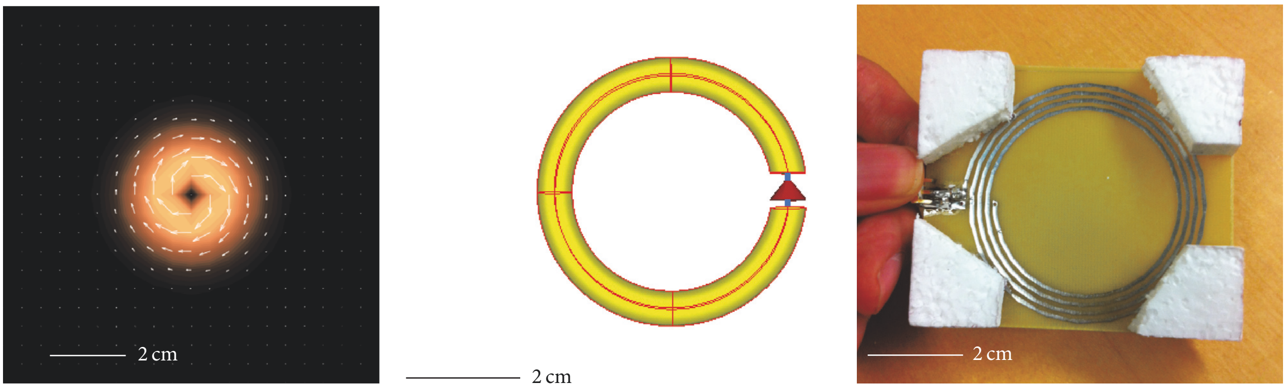

(a) (b) (c)

Figure 4: (a) The optimal current distribution for the frequency range of interest. (b) Simulated loop structure resembling the optimal source. (c) Fabricated loop structure with a matching network for the measurement.

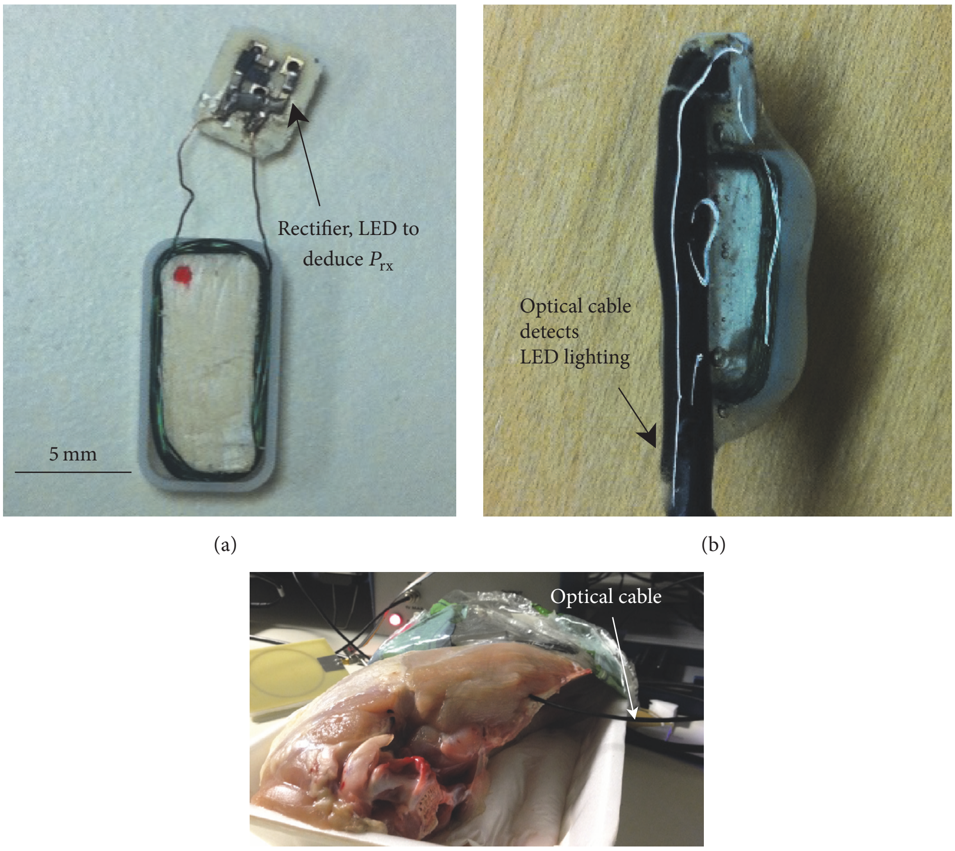
Rectifier, LED to deduce P_{rx}
5 mm
Optical cable detects LED lighting
Optical cable

(a) (b)

(c)

Figure 5: (a) Multiturn loop fits inside the same cover used in the ATI product. (b) Optical cable attached to detect LED lighting. (c) Turkey breast used for the experiment.

5. Conclusions

The theoretic bound of power transfer efficiency is derived for a centimeter-sized implantable device. Simulation is performed to verify the theory; guided by the theory, a power delivery system for a centimeter-sized neurostimulator in the head is designed. For this moderate-sized implant, the optimal frequency for power delivery system is at 15 MHz. Also, the optimal current distribution resembles that of a simple coil source, which is the most commonly used source structure for inductive coupling. Lastly, the experiment is performed for a receiver placed inside a turkey breast. The measured performance improves fivefold compared to that of the previous design.

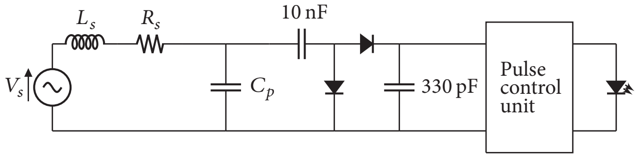

Figure 6: The circuit diagram of the receiver.

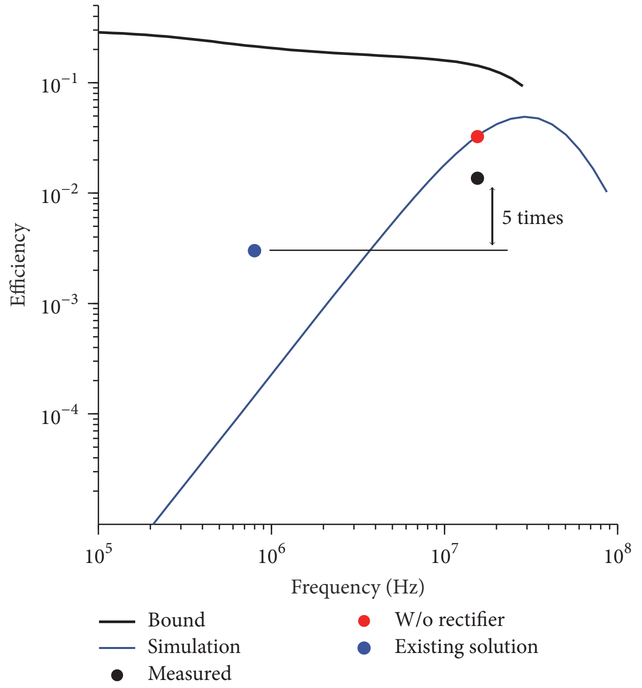

Figure 7: Measured power transfer efficiency versus the simulation and the bound. By increasing the operating frequency, the efficiency improved 5-fold compared to the existing solution.

Conflicts of Interest

The authors declare that they have no conflicts of interest.

Acknowledgments

This work was supported by grants from Kyung Hee University in 2016 (KHU-20160593).

References

[1] W. H. Ko, S. P. Liang, and C. D. F. Fung, “Design of radio-frequency powered coils for implant instruments,” *Medical and Biological Engineering and Computing*, vol. 15, no. 6, pp. 634–640, 1977.

[2] N. D. N. Donaldson and T. A. Perkins, “Analysis of resonant coupled coils in the design of radio frequency transcutaneous links,” *Medical & Biological Engineering & Computing*, vol. 21, no. 5, pp. 612–627, 1983.

[3] U. Jow and M. Ghovanloo, “Design and optimization of printed spiral coils for efficient transcutaneous inductive power transmission,” *IEEE Transactions on Biomedical Circuits and Systems*, vol. 1, no. 3, pp. 193–202, 2007.

[4] M. Kiani, U.-M. Jow, and M. Ghovanloo, “Design and optimization of a 3-coil inductive link for efficient wireless power transmission,” *IEEE Transactions on Biomedical Circuits and Systems*, vol. 5, no. 6, pp. 579–591, 2011.

[5] D. Kim and C. Seo, “Omnidirectional resonator in *X-Y* plane using a crisscross structure for wireless power transfer,” *Journal of Electromagnetic Engineering and Science*, vol. 15, no. 3, pp. 194–198, 2015.

[6] E. S. Hochmair, “System optimization for improved accuracy in transcutaneous signal and power transmission,” *IEEE Transactions on Biomedical Engineering*, vol. 31, no. 2, pp. 177–186, 1984.

[7] A. K. RamRakhyani, S. Mirabbasi, and M. Chiao, “Design and optimization of resonance-based efficient wireless power delivery systems for biomedical implants,” *IEEE Transactions on Biomedical Circuits and Systems*, vol. 5, no. 1, pp. 48–63, 2011.

[8] D. Ahn and M. Ghovanloo, “Optimal design of wireless power transmission links for millimeter-sized biomedical implants,” *IEEE Transactions on Biomedical Circuits and Systems*, vol. 10, no. 1, pp. 125–137, 2016.

[9] M. Q. Nguyen, Z. Hughes, P. Woods, Y.-S. Seo, S. Rao, and J.-C. Chiao, “Field distribution models of spiral coil for misalignment analysis in wireless power transfer systems,” *IEEE Transactions on Microwave Theory and Techniques*, vol. 62, no. 4, pp. 920–930, 2014.

[10] S. Kim, J. S. Ho, and A. S. Poon, “Wireless power transfer to miniature implants: transmitter optimization,” *IEEE Transactions on Antennas and Propagation*, vol. 60, no. 10, pp. 4838–4845, 2012.

[11] S. Kim, J. S. Ho, and A. S. Y. Poon, “Midfield wireless powering of subwavelength autonomous devices,” *Physical Review Letters*, vol. 110, no. 20, Article ID 203905, 2013.

[12] A. S. Y. Poon, S. O’Driscoll, and T. H. Meng, “Optimal frequency for wireless power transmission into dispersive tissue,” *IEEE Transactions on Antennas and Propagation*, vol. 58, no. 5, pp. 1739–1750, 2010.

[13] J. S. Ho, S. Kim, and A. S. Y. Poon, “Midfield wireless powering for implantable systems,” *Proceedings of the IEEE*, vol. 101, no. 6, pp. 1369–1378, 2013.

[14] J. S. Ho, A. J. Yeh, E. Neofytou et al., “Wireless power transfer to deep-tissue microimplants,” *Proceedings of the National Academy of Sciences of the United States of America*, vol. 111, no. 22, pp. 7974–7979, 2014.

[15] Autonomic technologies, http://www.ati-spg.com.

[16] S. Kim, J. S. Ho, L. Y. Chen, and A. S. Y. Poon, “Wireless power transfer to a cardiac implant,” *Applied Physics Letters*, vol. 101, no. 7, Article ID 073701, 2012.

[17] R. F. Harrington, *Time-Harmonic Electromagnetic Fields*, IEEE Press, 2001.

[18] We solve Maxwell’s equations for all physical sources using the method-of-moments (Mentor Graphics, IE3D).

[19] A. J. Yeh, J. S. Ho, and A. S. Y. Poon, “Optical probe for input-impedance measurement of in vivo power-receiving microstructure,” in *Proceedings of the IEEE Antennas and Propagation Society International Symposium (APSURSI ’14)*, pp. 1409-1410, Memphis, Tenn, USA, July 2014.

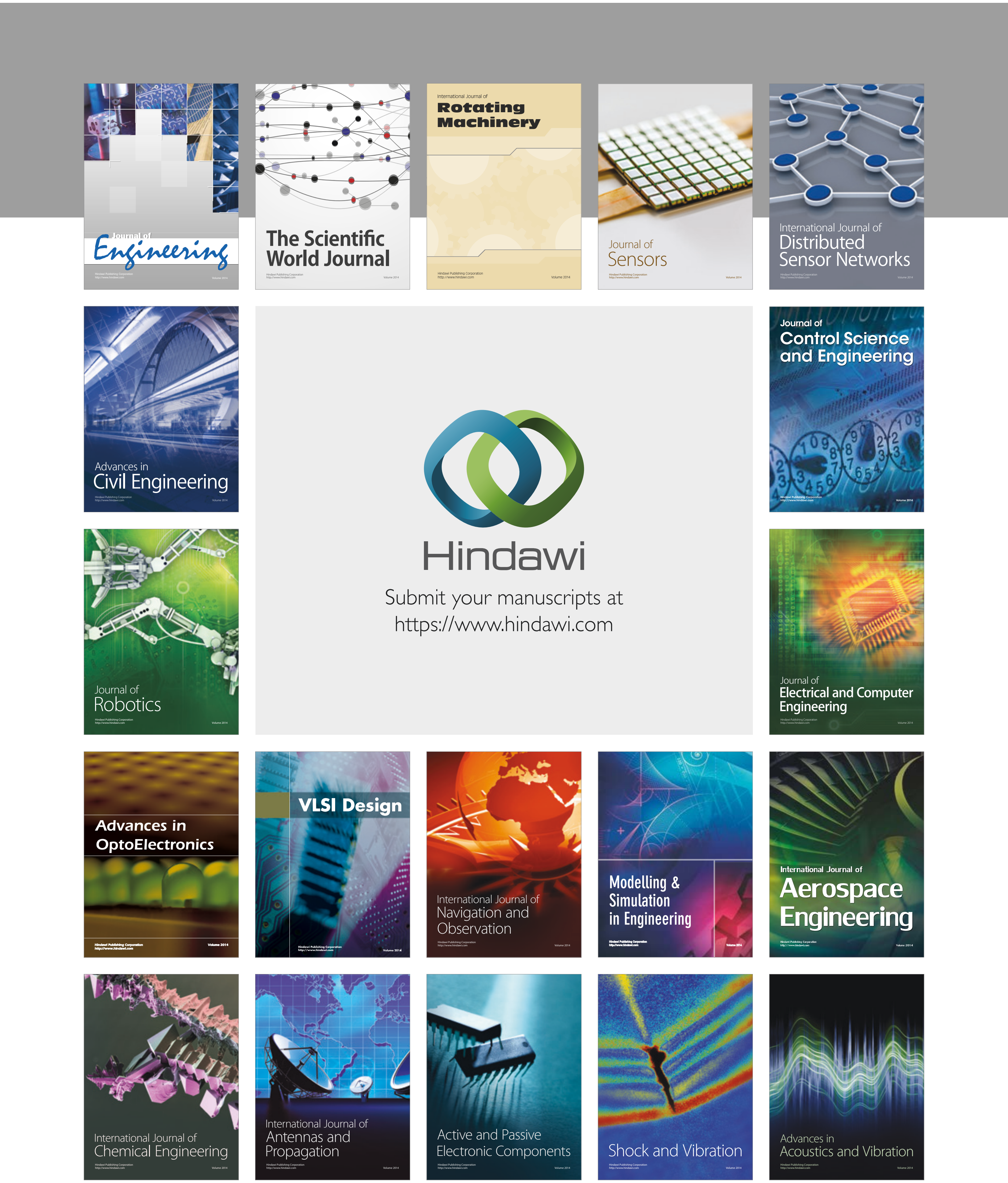

Hindawi

Submit your manuscripts at
https://www.hindawi.com

Journal of Engineering

The Scientific World Journal

International Journal of Rotating Machinery

Journal of Sensors

International Journal of Distributed Sensor Networks

Advances in Civil Engineering

Journal of Control Science and Engineering

Journal of Robotics

Journal of Electrical and Computer Engineering

Advances in OptoElectronics

VLSI Design

International Journal of Navigation and Observation

Modelling & Simulation in Engineering

International Journal of Aerospace Engineering

International Journal of Chemical Engineering

International Journal of Antennas and Propagation

Active and Passive Electronic Components

Shock and Vibration

Advances in Acoustics and Vibration